

# Comparison of two models for bridge-assisted charge transfer

M. Schreiber, D. Kilin, and U. Kleinekathöfer

*Institut für Physik, Technische Universität, D-09107 Chemnitz, Germany*

## Abstract

Based on the reduced density matrix method, we compare two different approaches to calculate the dynamics of the electron transfer in systems with donor, bridge, and acceptor. In the first approach a vibrational substructure is taken into account for each electronic state and the corresponding states are displaced along a common reaction coordinate. In the second approach it is assumed that vibrational relaxation is much faster than the electron transfer and therefore the states are modeled by electronic levels only. In both approaches the system is coupled to a bath of harmonic oscillators but the way of relaxation is quite different. The theory is applied to the electron transfer in  $\text{H}_2\text{P} - \text{ZnP} - \text{Q}$  with free-base porphyrin ( $\text{H}_2\text{P}$ ) being the donor, zinc porphyrin ( $\text{ZnP}$ ) being the bridge and quinone ( $\text{Q}$ ) the acceptor. The parameters are chosen as similar as possible for both approaches and the quality of the agreement is discussed.

## 1 Introduction

Long-range electron transfer (ET) is a very actively studied area in chemistry, biology, and physics; both in biological and synthetic systems. Of special interest are systems with a bridging molecule between donor and acceptor. For example the primary step of charge separation in the bacterial photosynthesis takes place in such a system [1]. But such systems are also interesting for synthesizing molecular wires [2]. It is known that the electronic structure of the bridge component in donor-bridge-acceptor systems plays a critical role [3, 4]. When the bridge energy is much higher than the donor and acceptor energies, the bridge population is close to zero for all times and the bridge site just mediates the coupling between donor and acceptor. This mechanism is called superexchange and was originally proposed by Kramers [5] to describe the exchange interaction between two paramagnetic atoms spatially separated by a nonmagnetic atom. In the opposite limit when donor and acceptor as well as bridge energies are closer than  $\sim k_{\text{B}}T$ , the bridge site is actually populated and the transfer is called sequential. The interplay between these two types of transfer has been investigated theoretically in various publications [1, 6, 7, 8, 9].

In the present work we compare two different approaches based on the reduced density matrix formalism. In the first model one pays attention to the fact that experiments in systems similar to the one discussed here show vibrational coherence [10, 11]. Therefore a vibrational substructure is introduced for each electronic level within a multi-level Redfield theory [12, 13]. Below we call this the vibronic model. In the second approach only electronic states are taken into account because it is assumed that the vibrational relaxation is much faster than the ET. This model is referred to as tight-binding model below. In this case only the relaxation between the electronic states remains. Such a kind of relaxation has been phenomenologically introduced for ET by Davis et al. [14]

and very recently derived in our group [15, 16] as a second order perturbation theory in the system-bath interaction similar to Redfield theory. The vibronic and the tight-binding model are described in the next section and compared in Section 3.

## 2 Theory

For the description of charge transfer and other dynamical processes in the system we introduce the Hamiltonian

$$\hat{H} = \hat{H}_S + \hat{H}_B + \hat{H}_{SB}, \quad (1)$$

where  $\hat{H}_S$  denotes the relevant system,  $\hat{H}_B$  the dissipative bath, and  $\hat{H}_{SB}$  the interaction between the two. Before discussing the system part of the Hamiltonian in Sections 2.1 and 2.2, we describe the bath and the procedure how to obtain the equations of motion for the reduced density matrix, because this is the same for both models studied below. The bath is modeled by a distribution of harmonic oscillators and characterized by its spectral density  $J(\omega)$ . Starting with a density matrix of the full system, the reduced density matrix of the relevant (sub)system is obtained by tracing out the bath degrees of freedom [17]. While doing so a second-order perturbation expansion in the system-bath coupling and the Markov approximation have been applied [17].

### 2.1 Vibronic model

The bridge ET system  $\text{H}_2\text{P} - \text{ZnP} - \text{Q}$  with free-base porphyrin ( $\text{H}_2\text{P}$ ) being the donor, zinc porphyrin ( $\text{ZnP}$ ) the bridge, and quinone ( $\text{Q}$ ) the acceptor is modeled by three diabatic electronic potentials, corresponding to the neutral excited electronic state  $|1\rangle = |\text{H}_2\text{P}^* - \text{ZnP} - \text{Q}\rangle$ , and states with charge separation  $|2\rangle = |\text{H}_2\text{P}^+ - \text{ZnP}^- - \text{Q}\rangle$ ,  $|3\rangle = |\text{H}_2\text{P}^+ - \text{ZnP} - \text{Q}^- \rangle$  (see Fig. 1). Each of these electronic potentials has a vibrational substructure. The vibrational frequency is assumed to be  $1500 \text{ cm}^{-1}$  as a typical frequency within carbon structures. The potentials are displaced along a common reaction coordinate which represents the solvent polarization [18]. Following the reasoning of Marcus [18] the free energy differences  $\Delta G_{mn}$  corresponding to the electron transfer from molecular block  $n$  to  $m$  ( $n = 1, m = 2, 3$ ) are estimated to be [19, 20]

$$\Delta G_{mn} = E_m^{\text{ox}} - E_n^{\text{red}} - E^{\text{ex}} - \frac{e^2}{4\pi\epsilon_0\epsilon_s} \frac{1}{r_{mn}} + \Delta G_{mn}(\epsilon_s) \quad (2)$$

with the term  $\Delta G_{mn}(\epsilon_s)$  correcting for the fact that the redox energies  $E_m^{\text{ox}}$  and  $E_n^{\text{red}}$  are measured in a reference solvent with dielectric constant  $\epsilon_s^{\text{ref}}$ :

$$\Delta G_{mn}(\epsilon_s) = \frac{e^2}{4\pi\epsilon_0} \left( \frac{1}{2r_m} + \frac{1}{2r_n} \right) \left( \frac{1}{\epsilon_s} - \frac{1}{\epsilon_s^{\text{ref}}} \right). \quad (3)$$

The excitation energy of the donor  $\text{H}_2\text{P} \rightarrow \text{H}_2\text{P}^*$  is denoted by  $E^{\text{ex}}$ .  $r_n$  denotes the radius of either donor (1), bridge (2), or acceptor (3) and  $r_{mn}$  the distance

between two of them. They are estimated to be  $r_1 = r_2 = 5.5 \text{ \AA}$ ,  $r_3 = 3.2 \text{ \AA}$ ,  $r_{12} = 12.5 \text{ \AA}$ , and  $r_{13} = 14.4 \text{ \AA}$  [19, 20].

Also sketched in Fig. 1 are the reorganization energies  $\lambda_{mn} = \lambda_{mn}^i + \lambda_{mn}^s$ . These consist of an internal reorganization energy  $\lambda_{mn}^i$ , which is estimated to be 0.3 eV [20], and a solvent reorganization energy [18]

$$\lambda_{mn}^s = \frac{e^2}{4\pi\epsilon_0} \left( \frac{1}{2r_m} + \frac{1}{2r_n} - \frac{1}{r_{mn}} \right) \left( \frac{1}{\epsilon_\infty} - \frac{1}{\epsilon_s} \right). \quad (4)$$

Further parameters are the electronic couplings between the potentials. First it should be underlined that  $V_{13} = 0$  because of the spatial separation of  $\text{H}_2\text{P}$  and  $\text{Q}$ . So there is no direct transfer between donor and acceptor. The other couplings are  $V_{12} = 65 \text{ meV}$  and  $V_{23} = 2.2 \text{ meV}$  [20]. The damping is described by the spectral density  $J(\omega)$  of the bath. This is only needed at the frequency of the vibrational transition and is determined  $J(\omega_{\text{vib}})/\omega_{\text{vib}} = 0.372$  by fitting the ET rate for the solvent methyltetrahydrofuran (MTHF). In the vibronic model the spectral density is taken as a constant with respect to  $\epsilon_s$ .

Next the calculation of the dynamics is sketched. Starting from the Liouville equation, performing the abovementioned approximations the equation of motion for the reduced density matrix  $\rho_{\mu\nu}$  can be obtained [12, 13]

$$\frac{\partial}{\partial t} \rho_{\mu\nu} = \frac{i}{\hbar} (E_\mu - E_\nu) \rho_{\mu\nu} - i \sum_{\kappa} \{v_{\nu\kappa} \rho_{\mu\kappa} - v_{\kappa\mu} \rho_{\kappa\nu}\} + R_{\mu\nu}. \quad (5)$$

The index  $\mu$  combines the electronic quantum number  $m$  and the vibrational quantum number  $M$  of the diabatic levels  $E_\mu$ .  $v_{\mu\nu} = V_{mn} F_{\text{FC}}(m, M, n, N)$  comprises Franck-Condon factors  $F_{\text{FC}}$  and the electronic matrix elements  $V_{mn}$ . The third term describes the interaction between the relevant system and the heat bath. Equation (5) is solved numerically with the initial condition that only the donor state is occupied in the beginning. The population of the acceptor state

$$P_3(t) = \sum_M \rho_{3M3M}(t) \quad (6)$$

and the ET rate

$$k_{\text{ET}} = \frac{P_3(\infty)}{\int_0^\infty dt (1 - P_3(t))} \quad (7)$$

are calculated by tracing out the vibrational modes.

## 2.2 Tight-binding model

The reasoning for the following system Hamiltonian is the assumption that the vibrational excitations are relaxed on a much shorter time scale than the ET time scale. Therefore only electronic states without any vibrational substructure are taken into account (see Fig. 2). As a consequence the relaxation during the ET process has to be described in a different manner than in the previous subsection. If now relaxation takes place, it takes place between the electronic states and not between vibrational states within one electronic state potential

surface. A similar model has been introduced phenomenologically by Davis et al. [14] who solved it in the steady state limit.

The energies of the electronic states  $E_m$  are chosen to be the ground states of the harmonic potentials given in the previous section. So they vary with the dielectric constant. The electronic coupling is fixed in two different ways. In the naive way they are chosen to be the same as in the vibronic model. But because in the tight-binding model there is no reaction coordinate, in a second version we scale the electronic couplings with the Franck-Condon overlap elements between the vibrational ground states of each pair of electronic surfaces

$$v_{mn} = V_{mn} F_{\text{FC}}(m, 0, n, 0) = V_{mn} \exp \frac{-|\lambda_{mn}|}{2\hbar\omega_{\text{vib}}} . \quad (8)$$

In the vibronic model not only the free energy differences  $\Delta G$  but also the reorganization energies  $\lambda$  scale with the dielectric constant  $\epsilon_s$ . Due to this scaling of  $\lambda$  the system-bath interaction is scaled with the dielectric constant  $\epsilon_s$ . In the high temperature limit the reorganization energy is given by [21]

$$\lambda = \hbar \int_0^\infty d\omega \frac{J(\omega)}{\omega} . \quad (9)$$

This relation is taken as motivation to scale the tight-binding spectral density with  $\epsilon_s$  like the reorganization energies  $\lambda$  in the vibronic model. In the present calculations  $\Gamma_{21} = \Gamma_{23} = \Gamma$  is assumed. The absolute value of the damping rate  $\Gamma$  between the electronic states (see Fig. 2) is then determined by fitting the ET rate for the solvent MTHF to be  $\Gamma = 2.8 \times 10^{11} \text{ s}^{-1}$ .

The advantage of the tight-binding model is the possibility to determine the transfer rate  $k_{\text{ET}}$  and the final population of the acceptor state either numerically or analytically. We employ the rotating wave approximation because we are only interested in the reaction rates here. For the analytic calculation three extra assumptions have to be made: small bridge population, the kinetic limit  $t \gg \Gamma^{-1}$ , and the absence of initial coherence in the system. But for all situations described in this paper the differences between analytic and numerical results without the extra assumptions are negligible. The analytic expressions are

$$k_{\text{ET}} = g_{23} + \frac{g_{23}(g_{12} - g_{32})}{g_{21} + g_{23}} \quad (10)$$

and

$$P_3(\infty) = \frac{g_{12}g_{23}}{g_{21} + g_{23}} (k_{\text{ET}})^{-1}, \quad (11)$$

which contain both, dissipative and coherent contributions

$$g_{mn} = d_{mn} + \frac{v_{mn}^2 \sum_k (d_{mk} + d_{kn})}{\hbar^2 \left\{ 2\omega_{mn}^2 + \frac{1}{2} \left[ \sum_k (d_{mk} + d_{kn}) \right]^2 \right\}} . \quad (12)$$

Herein the  $d_{mn}$  are just abbreviations for  $\Gamma_{mn}|n(\omega_{mn})|$  and  $n(\omega_{mn})$  denotes the Bose distribution at frequency  $\omega_{mn} = (E_m - E_n)/\hbar$ . For details and comparison with the Grover-Silbey theory [22] as well as the Haken-Strobl-Reineker theory [23] we refer the reader to Ref. [16].

### 3 Comparison

In Fig. 3 it is shown how the minima of the potential curves change with varying the solvent due to the changes in Eqs. (2) to (4). The solvents are listed in Table 1 together with their parameters and the results for the ET rates in both models. For larger  $\epsilon_s$  the coordinates of the potential minima of bridge and acceptor increase while their energies decrease with respect to the energy of the donor. The energy difference between donor and bridge decreases with increasing  $\epsilon_s$ . This makes a charge transfer more probable. For small  $\epsilon_s$  the acceptor state is higher in energy than the donor state; nevertheless there is a small ET rate due to coherent mixing.

For fixed  $\epsilon_\infty$  the ET rate is plotted as a function of the dielectric constant  $\epsilon_s$  in Fig. 4. The ET rate in the vibronic model increases strongly for small values of  $\epsilon_s$  while the increase is very small for  $\epsilon_s$  in the range between 5 and 8. The increase for small values of  $\epsilon_s$  is due to the fact that with increasing  $\epsilon_s$  the minimum of the acceptor potential moves from a position higher than the minimum of the donor level to a position lower than the donor level. So the transfer becomes energetically favorable. This can also be seen when looking at the results for the tight-binding model without scaling the electronic coupling with the Franck-Condon factor. In this case the ET rate increases almost linearly with increasing  $\epsilon_s$ . The effect missing in this model is the overlap between the vibrational states. If one corrects the electronic coupling in the tight-binding model by the Franck-Condon factor of the vibrational ground states as described in Eq. (8), good agreement is observed between the vibronic and the tight-binding model.

The ET rate for the vibronic model shows some oscillations as a function of  $\epsilon_s$ . This is due to the small density of vibrational levels in this model with one reaction coordinate. All three electronic potential curves are harmonic and have the same frequency. So there are small maxima in the rate when two vibrational levels are in resonance and minima when they are far off resonance. Models with more reaction coordinates do not have this problem nor does the simple tight-binding model. If these artificial oscillations would be absent, the agreement between the results for the tight-binding and the vibronic model would be even better, because the rate for the vibronic model happens to have a maximum just at the reference point  $\epsilon_s = 6.24$  which we have chosen to fix the spectral density, i. e. for MTHF.

The comparison of the two models has been made assuming that the scaling of energies as a function of the dielectric function is correct in the Marcus theory. There have been a lot of changes to Marcus theory proposed in the last years. Marcus theory assumes excess charges within cavities surrounded by a polarizable medium and there one only takes the leading order into account. Higher order terms are included in the so called reaction field theory (see for example [24]). But to compare different solvation models is out of the range of the present investigation. Some more details on this issue for the tight-binding model are given in Ref. [16]. Here we just want to note in passing that the effect of scaling the system-bath interaction with  $\epsilon_s$ , as assumed in the present work for the tight-binding model, has no big effect on the ET rates.

As conclusion we mention that one gets good agreement for the ET rates of the models with and without vibrational substructure, i. e. the vibronic and the tight-binding model, if one scales the electronic coupling with the Franck-Condon overlap matrix elements between the vibrational ground states. The advantage of the model with electronic relaxation only is the possibility to derive analytic expressions for the ET rate and the final population of the acceptor state. But of course for a more realistic description of the ET transfer process in such complicated systems as discussed here, more than one reaction coordinate should be taken into account. Work in this direction is in progress.

## 4 Acknowledgements

We thank I. Kondov for the help with some programming as well as U. Rempel and E. Zenkevich for stimulating discussions. Financial support of the DFG is gratefully acknowledged.

## References

- [1] M. Bixon, J. Jortner and M. E. Michel-Beyerle, *Biochim. Biophys. Acta* 1056 (1991) 301; *Chem. Phys.* 197 (1995) 389.
- [2] W. B. Davis, W. A. Svec, M. A. Ratner, and M. R. Wasielewski, *Nature* 396 (1998) 60.
- [3] M. R. Wasielewski, *Chem. Rev.* 92 (1992) 345.
- [4] P. F. Barbara, T. J. Meyer, and M. A. Ratner, *J. Phys. Chem.* 100 (1996) 13148.
- [5] H. A. Kramers, *Physica* 1 (1934) 182.
- [6] H. Sumi and T. Kakitani, *Chem. Phys. Lett.* 252 (1996) 85; H. Sumi, *J. Electroan. Chem.* 438 (1997) 11.
- [7] A. K. Felts, W. T. Pollard, and R. A. Friesner, *J. Phys. Chem.* 99 (1995) 2929.
- [8] A. Okada, V. Chernyak, and S. Mukamel, *J. Phys. Chem. A* 102 (1998) 1241.
- [9] M. Schreiber, C. Fuchs, and R. Scholz, *J. Lumin.* 76&77 (1998) 482.
- [10] M. H. Vos, F. Rappaport, J.-C. Lambry, J. Breton, and J.-L. Martin, *Nature* 363 (1993) 320.
- [11] R. J. Stanley and S. G. Boxer, *J. Phys. Chem.* 99 (1995) 859.
- [12] V. May and M. Schreiber, *Phys. Rev. A* 45 (1992) 2868.
- [13] O. Kühn, V. May, and M. Schreiber, *J. Chem. Phys.* 101 (1994) 10404.

- [14] W. Davis, M. Wasilewski, M. Ratner, V. Mujica, and A. Nitzan, *J. Phys. Chem.* 101 (1997) 6158.
- [15] M. Schreiber, D. Kilin, and U. Kleinekathöfer, in: R. T. Williams and W. M. Yen (Eds.), *Excitonic Processes in Condensed Matter*, PV 98-25, p. 99, The Electrochemical Society Proceedings Series, Pennington, NJ, 1998.
- [16] D. Kilin, U. Kleinekathöfer, and M. Schreiber (in preparation).
- [17] K. Blum, *Density Matrix Theory and Applications*, Plenum Press, New York, 1996, 2nd ed.
- [18] R. A. Marcus, *J. Chem. Phys.* 24 (1956) 966; R. A. Marcus und N. Sutin, *Biochim. Biophys. Acta* 811 (1985) 265.
- [19] C. Fuchs, Ph.D. thesis, Technische Universität Chemnitz, 1997, <http://archiv.tu-chemnitz.de/pub/1997/0009>
- [20] U. Rempel, B. von Maltzan, and C. von Borczyskowski, *Chem. Phys. Lett.* 245 (1995) 253.
- [21] U. Weiss, *Quantum Dissipative Systems*, World Scientific, Singapore, 1999.
- [22] M. Grover and R. Silbey, *J. Chem. Phys.* 54 (1971) 4843.
- [23] P. Reineker, in: G. Höhler (Ed.), *Exciton Dynamics in Molecular Crystals and Aggregates*, Springer, Berlin, 1982.
- [24] M. Karelson, G. H. F. Diercksen, in: S. Wilson and G. H. F. Diercksen, *Problem Solving in Computational Molecular Science: Molecules in Different Environments*, Kluwer, Dordrecht, 1997.
- [25] Charles Tennant & Company (London) Ltd, <http://www.ctennant.co.uk/tenn04.htm>
- [26] J. A. Schmidt, J.-Y. Liu, J. R. Bolton, M. D. Archer, and V. P. Y. Gadzepko, *J. Chem. Soc. Faraday Trans.* 85 (1989) 1027.

solvent	$\epsilon_s$	$\epsilon_\infty$	$\Delta G_{21}$ [eV]	$\Delta G_{31}$ [eV]	$\lambda_{21}^s$ [eV]	$\lambda_{31}^s$ [eV]	$\Gamma$ [ $10^{11} \text{ s}^{-1}$ ]	$k_{\text{ET}}^{\text{el}}$ [ $10^8 \text{ s}^{-1}$ ]	$k_{\text{ET}}^{\text{vib}}$ [ $10^8 \text{ s}^{-1}$ ]
1. cyclohexane [20]	2.02	2.00	0.976	0.393	0.007	0.012	0.042	0.181	0.7
2. toluene [25]	2.38	2.24	0.867	0.202	0.039	0.069	0.227	1.04	0.8
3. anisole [26]	4.33	2.29	0.590	-0.281	0.300	0.524	1.751	4.24	2.30
4. dibromoethane [26]	4.78	2.37	0.558	-0.336	0.312	0.544	1.817	4.63	2.45
5. chlorobenzene [25]	5.29	1.93	0.529	-0.388	0.481	0.839	2.804	3.21	3.63
6. MTHF [20]	6.24	2.00	0.486	-0.462	0.497	0.868	2.900	3.59	3.58
7. methyl acetate [25]	6.68	1.85	0.471	-0.489	0.571	0.996	3.328	2.96	4.15
8. trichloroethane [26]	7.25	2.06	0.454	-0.512	0.508	0.887	2.960	3.98	3.50
9. dichloromethane [20]	9.08	2.03	0.413	-0.590	0.559	0.977	3.264	4.00	3.80

Table 1: Parameters and obtained transfer rates for different solvents. The references behind the names of the solvents cite the sources of  $\epsilon_s$  and  $\epsilon_\infty$ . MTHF stands for methyltetrahydrofuran.  $\Gamma$  denotes the damping rate in the tight-binding model. The ET rate for the solvent MTHF has been used to fix the damping parameter of the models. The reaction rates  $k_{\text{ET}}^{\text{el}}$  were obtained using Eq. (10) within the tight-binding model and the reaction rates  $k_{\text{ET}}^{\text{vib}}$  within the vibronic model.



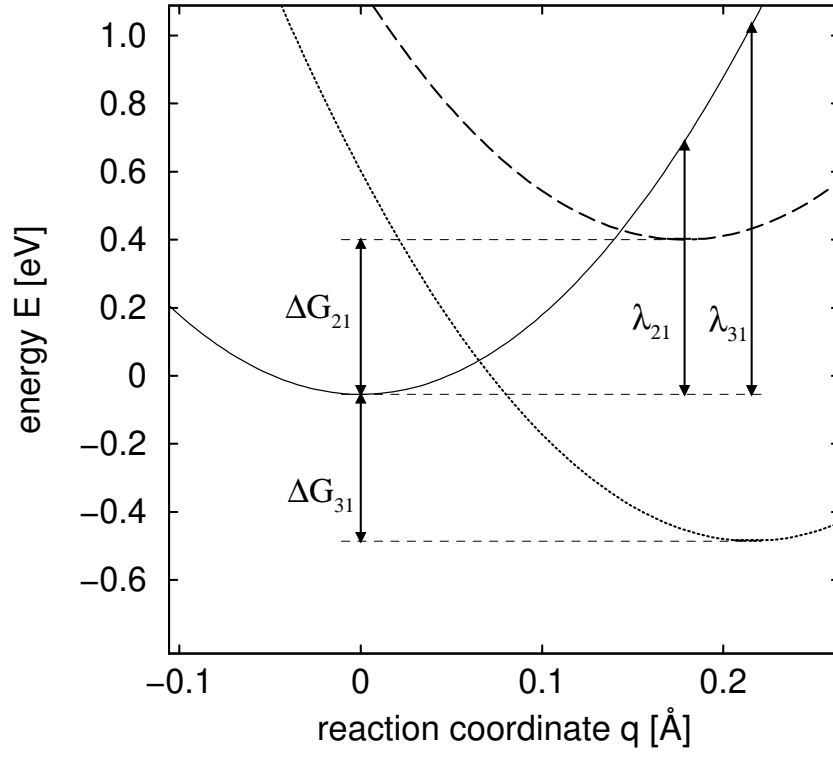


Figure 1: Electronic potentials and parameters of the vibronic model. The donor surface  $|\text{H}_2\text{P}^* - \text{ZnP} - \text{Q}\rangle$  is given by the solid line, the bridge  $|\text{H}_2\text{P}^+ - \text{ZnP}^- - \text{Q}\rangle$  by the dashed line, and the acceptor  $|\text{H}_2\text{P}^+ - \text{ZnP} - \text{Q}^-\rangle$  by the dotted line.

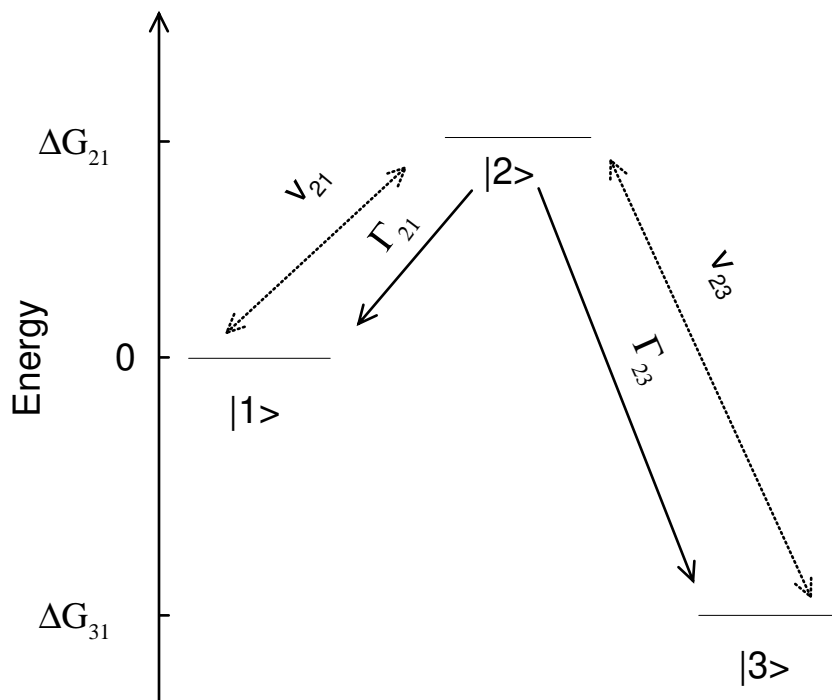


Figure 2: Schematic presentation of the tight-binding model.

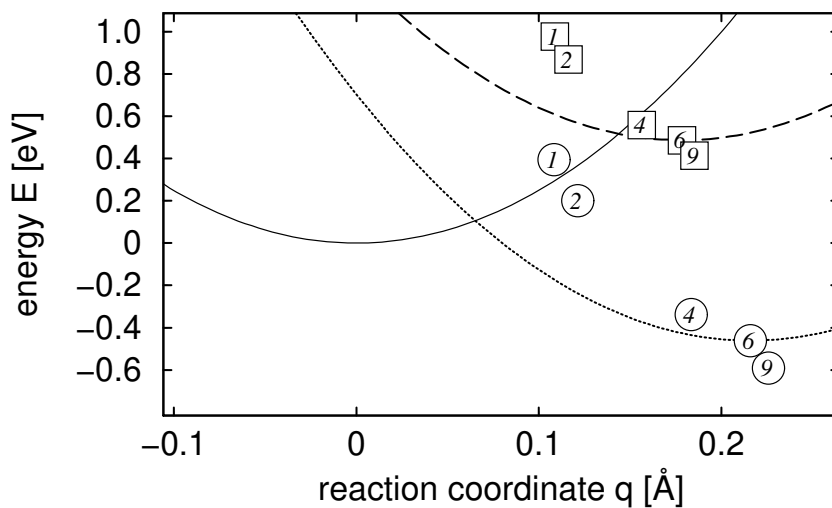


Figure 3: Variation of the potential minima for different solvents. Squares denote the bridge minima, circles the acceptor minima. The numbers correspond to the ordinal numbers in Table 1. The potentials are shown for solvent 6 (MTHF).

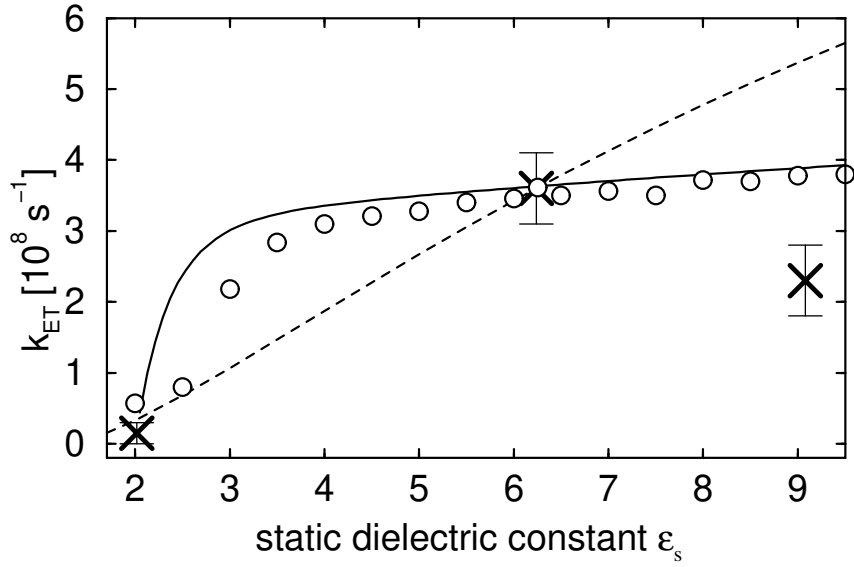


Figure 4: Transfer rate as a function of the dielectric constant  $\epsilon_s$  for both models together with experimental results [20]. The rates for the vibronic model are given by the circles. The dashed line shows the rate for the tight-binding model with electronic couplings  $V_{mn}$  as in the vibronic model. The solid line represents the rate for the tight-binding model with  $v_{mn}$  scaled as given in Eq. (8).